The skateboard speed wobble

Marco Rosatello, Jean-Luc Dion, Franck Renaud, Luigi Garibaldi

THE SKATEBOARD SPEED WOBBLE

Marco Rosatello
LISSMA
SUPMECA
Saint-Ouen, France 93400
Email: marco.rosatello@gmail.com

Jean-Luc Dion, Franck Renaud
LISSMA
SUPMECA
Saint-Ouen, France 93400

Luigi Garibaldi
DIMEAS
Polytechnic of Turin
Torino, Italy 10129

ABSTRACT

The speed wobble is a phenomenon in nonlinear dynamics that can occur in many vehicles such as bicycles, motorbikes, skateboards and airplanes nose landing gear. The dynamic instability affects the steerable wheels of a vehicle and can lead to the loss of control. While for bikes, motorbikes and airplanes the dynamics and causes of the wobble are well known and the literature fully describes the subject, for the skateboard the literature is very poor and there is no paper which investigates this type of instability.

In order to do that, the skateboard equations of motion were obtained through Lagrange formalism and Lagrange multipliers method was used to solve the non-holonomic constraints. A parametric stability study was carried out on the linearized equations of motion and the influence of different skateboard parameters was investigated.

The main discovery is that the wobble doesn't strictly depend on skateboard configuration, but the human control characteristics are predominant in the vehicle dynamics.

Keywords: wobble, skateboard, stability

NOMENCLATURE

a Skateboard wheelbase
COM Center of Mass
μ Ratio between front and rear truck torsional stiffness
γ Board tilt
h Board height from axles plane
I_{B_x} Board moment of inertia about x-axis
I_{R_x} Rider moment of inertia about x-axis
I_{B_z} Board moment of inertia about z-axis
I_{R_z} Rider moment of inertia about z-axis
λ_f Pivot angle front truck
λ_r Pivot angle rear truck
k_γ Overall skateboard truck torsional stiffness
k_{γ_f} Front truck torsional stiffness
k_{γ_r} Rear truck torsional stiffness
l Rider COM height from board
m_B Skateboard mass
m_R Rider mass
p Distance from the board center of the COM projection
T_B Total ankles torque
W_s Somatosensory weighting factor
W_v Visual+Vestibular weighting factor
u Longitudinal skateboard speed

INTRODUCTION

The skateboard is a recreational vehicle whose origin extend back to the early 20's, when it consisted of a rudimentary crate scooter made of a wooden board, metal wheels and a wooden box. In the 50's the first commercially produced skateboards appeared on the market. The very turning point in the skateboard history took place in the 70's, thanks to the use of polyurethane wheels, which allowed more controllability and traction properties than the previous metal wheels. They also allowed higher

speeds which brought to the emergence of a new type of skateboard, called longboard, specially designed for downhill skateboarding. They are longer than normal skateboards, they have different shapes and very high speed can be reached. The fastest skateboard speed achieved in a standing position is 129.94 km/h (80.74 mph) and was achieved by Mischo Erban at Les boulements, Quebec, Canada, on 18 June 2012 on a road descending at an 18% grade.
To achieve high speeds the skateboard has to be set up correctly and the rider has to adapt his body to control the vehicle. If one of the this two aspects fails, at a certain speed the skateboard-rider system can become unstable, showing an oscillatory behavior that can lead to loss of control and very dangerous falls. This phenomenon is known as *speed wobble*.

Literature Review

The existing literature about skateboard is limited and the speed wobble has never been treated. In [1] Hubbard studied the lateral dynamics stability of a 1-DOF and a 2-DOF linearized skateboard model, but the speed wobble is not treated.
Again Hubbard, in [2], after simplifying hypotheses and reducing the 2-DOF model to a 1-DOF model, implemented an optimal control to the skateboard in order to simulate the human control. However, even if the perfect control has been experimentally verified to be similar to the actual human control for low speeds, it's not interesting for higher speed ranges.
Another major work in the skateboard field is [3], in which Kremnev and Kuleshov, on the basis of [1], study the stability of a more accurate 1 DOF skateboard model, obtaining the equations of motion through the Gibbs-Appell method. They offer a mathematically accurate nonlinear stability analysis, demonstrating a rattleback behavior for asymmetric skateboards around the equilibrium position. However, the speed wobble is never mentioned.
The objective of this paper is to study the skateboard stability in a speed-wobble-focused way, analyzing the most affecting parameters, and to verify or disprove common skaters beliefs about speed wobble. In order to do that, a parametric stability analysis will be carried out on a 1 DOF skateboard model, with the intention of determining the parameters that has more influence on stability at higher speeds. Furthermore, a human control model based on Biomechanics researches on the human postural control (see [10]- [16]) will be implemented on a second model of skateboard.

THE SKATEBOARD

The skateboard typically consists of three major components: a board, a set of two trucks and four wheels. A skateboard model is shown in Fig.1. Modern boards are generally from 50 to 110 cm long, 15 to 30 cm wide and 1 to 2 cm thick. The stiffness of the board depends on the particular application desired:

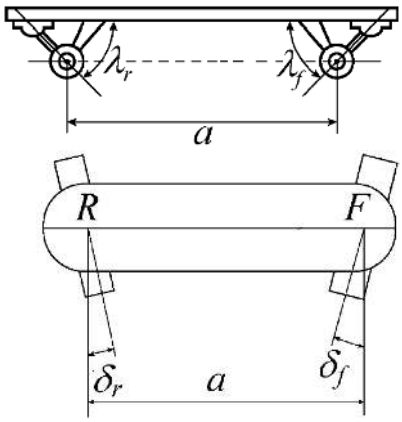

FIGURE 1: LATERAL AND TOP VIEW OF A SKATEBOARD

when a great manoeuvrability is required, a more flexible board is used, while stability at high speeds calls for more stiffness. In this study the board stiffness won't be considered in the equations of motion. The skateboard wheels are mounted on the axles on ball bearings and their stiffness is measured with the durometer A scale. The range of commercial wheels hardness is between 75A and 97A. Concerning the trucks, they are the elements that allow the skateboard to turn. The most common model is called Randal truck and it is characterized by three parameters: the wheelbase a, the pivot angle λ and the bushings.
The wheelbase a is simply the distance between the front and rear truck. The pivot angle λ is the angle between the baseplate and the kingpin. The front truck pivot angle is λ_f, while the rear one λ_r, as shown in Fig.1. Normally the mounted trucks are the same, thus $\lambda_f = \lambda_r$, but sometimes different configurations are used. The bushings exist in different shapes and hardness and, together with the tightening of the kingpin bolt, they determine the overall torsional spring stiffness k_γ, shown in Fig.3. The latter applies a restoring torque T_γ between the wheel-set and the board, proportional to the tilt angle γ.
In [1–5], the effect of different trucks tightening is not taken into account. In this study we will consider the possibility that the front and rear truck torsional spring levels of stiffness k_{γ_F} and k_{γ_R} are different, which is a very common set up among skaters. We can write the overall restoring torque as

$$T_\gamma = k_\gamma \gamma = k_{\gamma_f} \gamma_f + k_{\gamma_r} \gamma_r \tag{1}$$

where γ_f andγ_r are the board tilt angles at the points F and R shown in Fig.1. Assuming that

$$k_{\gamma_f} \gamma_f = k_{\gamma_r} \gamma_r \tag{2}$$

and by replacing (2) in (1),we can find

$$\gamma_f = \frac{1+\mu}{2\mu}\gamma \qquad \gamma_r = \frac{1+\mu}{2}\gamma \tag{3}$$

where $\mu = k_{\gamma_f}/k_{\gamma_r}$.

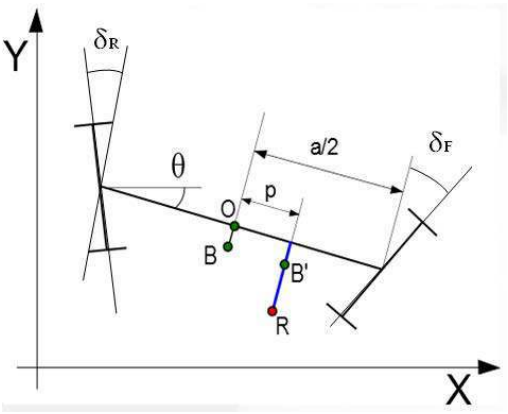

FIGURE 2: SKATEBOARD COORDINATE SYSTEM

Steering system

The skateboard is a negative-four wheel steering vehicle (for more details see [6]): the angular motion of both the front and rear axles is constrained to be about their respective pivot axes, thus causing steering angles δ_f and δ_r, shown in Fig.2, whenever the axles are not parallel to the plane of the board. The relationship between the board tilt angle γ and the steering angles δ_f and δ_r has been demonstrated in [3] to be

$$\tan\delta_f = \tan\lambda_f \sin\gamma \qquad \tan\delta_r = \tan\lambda_r \sin\gamma \tag{4}$$

Once the trucks are mounted, the pivot angles λ_f and λ_r are fixed. Furthermore taking into account (3), (4) becomes

$$\tan\delta_f = c_f \sin\left(\frac{1+\mu}{2\mu}\gamma\right) \qquad \tan\delta_r = c_r \sin\left(\frac{1+\mu}{2}\gamma\right) \tag{5}$$

where $c_f = \tan\lambda_f$ and $c_r = \tan\lambda_r$. The last step to fully define the skateboard steering system is to assume that its wheels roll without lateral sliding. Looking at Fig.2, this condition is satisfied through two nonholonomic constraints defined in [3] as:

$$\begin{aligned} \dot{x}_o \sin(\theta-\delta_f) - \dot{y}_o \cos(\theta-\delta_f) - \frac{a}{2}\dot{\theta}\cos\delta_f = 0 \\ \dot{x}_o \sin(\theta+\delta_r) - \dot{y}_o \cos(\theta+\delta_r) + \frac{a}{2}\dot{\theta}\cos\delta_r = 0 \end{aligned} \tag{6}$$

EQUATIONS OF MOTION

The skateboard equations of motion are obtained for two different models with different assumptions. In Model 1, outlined in Fig.3, the rider is assumed to remain fixed and perpendicular to the board, so that the angle between the z-axis and the rider COM is the same board tilt angle γ.
In Model 2, outlined in Fig.4, the rider is assumed to move freely about the x-axis, thus forming an angle ϕ between the rider COM and the vertical z-axis. The rider is assumed to control its position through a torque exerted at the ankles level about the axis passing from the center of the board. In both models, when $\gamma = 0$, the projection of the rider COM is assumed to lie on the board centerline $\overline{FR}$ at a distance p from the board center B,as shown in Fig.2. If $p > 0$ the rider COM is shifted in the front of the vehicle, while if $p < 0$ in the back. The equations of motion are obtained through Lagrange formalism with Lagrange multipliers to account for the nonholonomic constraints (6).
Choosing the vector of N Lagrangian generalized coordinates $q = (q_1, q_2, ..., q_N)^T$, the Lagrange energy method allows to write the equations of motion from the kinetic energy T and potential energy U expressions for the system under investigation. Being N_C the number of constraints and

$$\sum_{i=1}^{N} c_{ji}(q)\cdot\dot{q}_i = 0 \quad , \quad j = 1, ..., N_C \tag{7}$$

the resulting first-order differential equations in Pfaffian form, following [7], the equations of motion with N_C Lagrange multipliers λ can be written as

$$\frac{d}{dt}\frac{\partial L(q,\dot{q})}{\partial \dot{q}_i} - \frac{\partial L(q,\dot{q})}{\partial q_i} = Q_i + \sum_{j=1}^{N_C} \lambda_j c_{ji}(q) \quad i = 1, .., N \tag{8}$$

where $L(q,\dot{q}) = T(q,\dot{q}) - U(q)$ is called Lagrangian,Q_i contains the generalized forcing terms f_i and the dissipative forces terms d_i.
The second-order differential system of equations (8) and the first-order differential system of equations (7) give a total of $N + N_C$ equations for computation of the $N + N_C$ unknowns $q_1, q_2, ..., q_N$ and $\lambda_1, ..., \lambda_{N_C}$. Here the Lagrange multipliers represent the constraint forces required to maintain the constraints in Eq.(7).
The final first-order differential system of equations is:

$$\begin{bmatrix} I & 0 & 0 \\ 0 & A & C^T \\ 0 & C & 0 \end{bmatrix} \begin{bmatrix} \dot{q} \\ \ddot{q} \\ -\lambda \end{bmatrix} = \begin{bmatrix} \dot{q} \\ Q(\dot{q},q,t) + B(\dot{q},q,t) \\ D(\dot{q},q,t) \end{bmatrix} \tag{9}$$

where

$$D(\dot{q},q,t) = C\ddot{q} \tag{10}$$

on which the Baumgarte stabilization method have been applied.

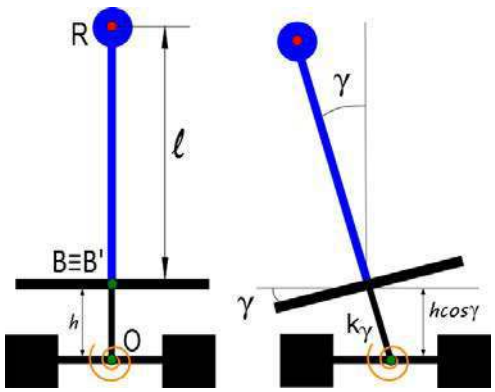

FIGURE 3: FRONT VIEW OF MODEL 1

Model 1 - Rider Constrained

The generalized coordinate vector for Model 1 is: $q = [x_O, y_O, \theta, \gamma]$, where x_O and y_O are the coordinates of point O, shown in Fig.2,3. Considering a skateboard with a mass m_B, moments of inertia I_{B_x} , I_{B_z} and its COM in point B and a rider with a mass m_R, moments of inertia I_{R_x} , I_{R_z} and its COM in point R, the expression of the kinetic energy is:

$$T = \frac{1}{2}m_B(\dot{x}_B^2 + \dot{y}_B^2 + \dot{z}_B^2) + \frac{1}{2}m_R(\dot{x}_R^2 + \dot{y}_R^2 + \dot{z}_R^2) + \frac{1}{2}I_x\dot{\gamma}^2 + \frac{1}{2}I_z\dot{\theta}^2 \quad (11)$$

where $I_x = I_{B_x} + I_{R_x}$ and $I_z = I_{B_z} + I_{R_z}$, since the rotational speeds $\dot{\gamma}$ and $\dot{\theta}$ are the same for the board and the rider. The potential energy is:

$$U = \frac{1}{2}k_\gamma\gamma^2 + m_B g z_B + m_R g z_R \quad (12)$$

Concerning the generalized forces, there are no active forces or torques acting on the skateboard, thus the generalized forces vector is $Q_1 = [0,0,0,0]^T$.
In order to write Eq.(11) and (12) as function of the generalized coordinates, looking at Figs.2-3, the following geometric constraints were found:

$$\begin{aligned} x_B &= x_O + h\sin\gamma\sin\theta \;,\; x_R = x_O + (h+l)\sin\gamma\sin\theta + p\cos\theta \\ y_B &= y_O - h\sin\gamma\cos\theta \;,\; y_R = y_O - (h+l)\sin\gamma\cos\theta + p\sin\theta \\ z_B &= h\cos\gamma \;,\; z_R = (h+l)\cos\gamma \end{aligned} \quad (13)$$

and deriving them in respect of time we obtain

$$\begin{aligned} \dot{x}_B &= \dot{x}_O + h(\dot{\gamma}\cos\gamma\sin\theta + \dot{\theta}\sin\gamma\cos\theta) \\ \dot{x}_R &= \dot{x}_O + (h+l)(\dot{\gamma}\cos\gamma\sin\theta + \dot{\theta}\sin\gamma\cos\theta) - p\dot{\theta}\sin\theta \\ \dot{y}_B &= \dot{y}_O - h(\dot{\gamma}\cos\gamma\cos\theta + \dot{\theta}\sin\gamma\sin\theta) \\ \dot{y}_R &= \dot{y}_O - (h+l)(\dot{\gamma}\cos\gamma\cos\theta + \dot{\theta}\sin\gamma\sin\theta) + p\dot{\theta}\cos\theta \\ \dot{z}_B &= -h\dot{\gamma}\sin\gamma \;,\; \dot{z}_R = -(h+l)\dot{\gamma}\sin\gamma \end{aligned} \quad (14)$$

Then we replace (14) and (13) in (11) and (12) At this point the first-order differential system (9) was derived with the Symbolic Math Toolbox of MATLAB®. The resulting matrices are omitted for brevity.

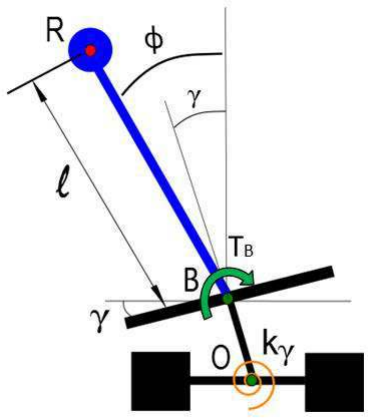

FIGURE 4: FRONT VIEW OF MODEL 2

TABLE 1: AVERAGE SKATEBOARD-RIDER DATA

Skateboard - Rider Parameters					
m_B	3	kg	m_R	75	kg
a	0.6	m	l	0.7	m
λ_f	45	°	λ_r	45	°
h	0.07	m	p	0	m
I_{B_x}	0.025	kgm^2	I_{B_x}	12	kgm^2
m_f	3	kg	I_{fx}	0.45	kgm^2
k_γ	250	$Nm\,rad^{-1}$	μ	1	

Model 2

The same procedure is followed for Model 2. The outline of the model is shown in Fig.4. Concerning the human control, the latter is exerted through an ankles torque T_B, assumed to act around the board x-axis.
The generalized coordinate vector is $q = [x_O, y_O, \theta, \gamma, \phi]$.
Since in this model the rider is assumed to move independently of the board, some considerations have to be made on the inertia terms. In particular it's important to pay attention to the feet inertia. In fact, even if the skater body moves independently of the board, the feet are fixed to the board and their rotation is equal to the board tilt angle γ and not the skater COM angle ϕ. Therefore, the feet inertia around the x-axis I_{fx} has to be considered with the board inertia and not with the rider inertia.
In the same way also the mass of the feet has to be considered with the board so that:

$$m'_B = m_B + m_f \quad , \quad m'_R = m_R - m_f \quad (15)$$

While the new inertia terms becomes then:

$$I'_{B_x} = I_{B_x} + I_{fx} \quad , \quad I'_{R_x} = I_{R_x} - I_{fx} \quad (16)$$

The expression of the kinetic energy is:

$$\begin{aligned} T = &\frac{1}{2}m_B(\dot{x}_B^2 + \dot{y}_B^2 + \dot{z}_B^2) + \frac{1}{2}m_R(\dot{x}_R^2 + \dot{y}_R^2 + \dot{z}_R^2) \\ &+ \frac{1}{2}I'_{B_x}\dot{\gamma}^2 + \frac{1}{2}I'_{R_x}\dot{\phi}^2 + \frac{1}{2}I_z\dot{\theta}^2 \end{aligned} \quad (17)$$

while the potential energy is:

$$U = \frac{1}{2}k_\gamma\gamma^2 + \frac{1}{2}k_\phi(\gamma-\phi)^2 + m_B g z_B + m_R g z_R \quad (18)$$

Concerning the generalized forces, the only active force is the ankle torque exerted by the skater, so that the vector of generalized forces becomes $Q_2 = [0,0,0,-T_B,T_B]^T$.
Concerning the geometric constraints, for the point B they remain the same as for Model 1, while for point R they become:

$$\begin{aligned} x_R &= x_O + (h\sin\gamma + l\sin\phi)\sin\theta + p\cos\theta \\ y_R &= y_O - (h\sin\gamma + l\sin\phi)\cos\theta + p\sin\theta \\ z_R &= h\cos\gamma + l\cos\phi \end{aligned} \quad (19)$$

while their derivatives become:

$$\begin{aligned}
\dot{x}_R &= \dot{x}_O + (h\dot{\gamma}\cos\gamma + l\dot{\phi}\cos\phi - p\dot{\theta})\sin\theta + \dot{\theta}(h\sin\gamma + l\sin\phi)\cos\theta \\
\dot{y}_R &= \dot{y}_O - (h\dot{\gamma}\cos\gamma + l\dot{\phi}\cos\phi - p\dot{\theta})\cos\theta + \dot{\theta}(h\sin\gamma + l\sin\phi)\sin\theta \\
\dot{z}_R &= -h\dot{\gamma}\sin\gamma - l\dot{\phi}\sin\phi
\end{aligned} \tag{20}$$

Linearized Equations

To linearize the equations of motion several assumptions are made. The longitudinal speed $\dot{x}_O$ is assumed to have a constant value u so that $\ddot{x}_O = 0$.
From [3] is demonstrated that

$$\dot{\theta} = -\frac{u\sin(\delta_f + \delta_r)}{a\cos\delta_f\cos\delta_r} \tag{21}$$

and that, solving the two nonholonomic constraints (6) is possible to find

$$\dot{y}_O = -\frac{a\dot{\theta}}{2\sin(\delta_f + \delta_r)}[\cos\delta_f\sin(\theta + \delta_r) + \cos\delta_r\sin(\theta - \delta_f)] \tag{22}$$

Furthermore, small angles assumption is made for the angles γ,θ and ϕ, so that $\cos\gamma = \cos\theta = \cos\phi \simeq 1$, $\sin\gamma \simeq \gamma$, $\sin\theta \simeq \theta$, $\sin\phi \simeq \phi$.
Taking into account the assumption made and replacing (21),(22) and their time derivatives in system (9), we obtain the linearized equation for Model 1:

$$\begin{aligned}
&\left(I_x + m_R L^2 + m_B h^2\right)\ddot{\gamma} + \left[m_R L\left(\varepsilon + \eta\frac{p}{a}\right) + m_B h\varepsilon\right]u\dot{\gamma} \\
&+ \left[k_\gamma - m_R g L - m_B g h + \frac{\eta u^2}{a}(m_R L + m_B h)\right]\gamma = 0
\end{aligned} \tag{23}$$

where $L = h + l$,while

$$\varepsilon = \frac{\mu+1}{4\mu}(c_f - c_r\mu) \quad , \quad \eta = \frac{\mu+1}{2\mu}(c_f + c_r\mu) \tag{24}$$

are the coefficients that take into account the eventuality of different trucks pivot angles and degrees of stiffness. They act as damping parameters but they don't involve any viscoelastic behavior of the trucks bushings.
The linearized system of equations for Model 2 is

$$\begin{aligned}
&\left(I'_{B_x} + mh^2\right)\ddot{\gamma} + m'_R hl\ddot{\phi} + \left(m\varepsilon + m'_B\eta\frac{p}{a}\right)hu\dot{\gamma} \\
&+ \left(k_\gamma - mgh + mh\frac{\eta u^2}{a}\right)\gamma = -T_B \\
&\left(I'_{R_x} + m_r l^2\right)\ddot{\phi} + m'_R hl\ddot{\gamma} + \left[m'_R l\left(\varepsilon + \eta\frac{p}{a}\right)\right]u\dot{\gamma} \\
&- m'_R gl\phi + m'_R\frac{l\eta u^2}{a}\gamma = T_B
\end{aligned} \tag{25}$$

where $m = m_R + m_B$.

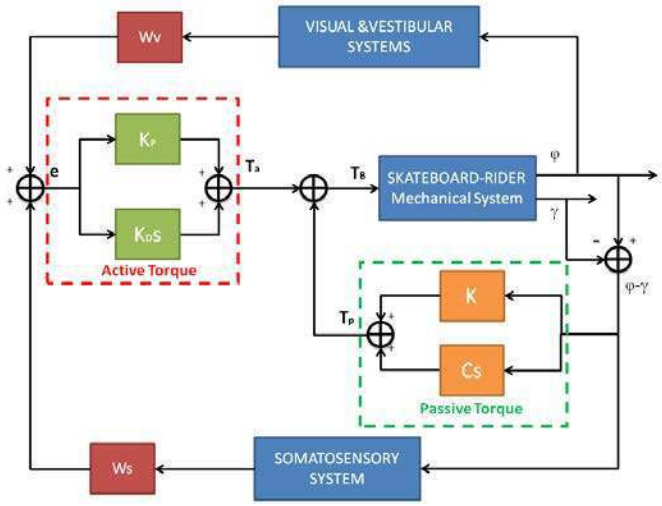

FIGURE 5: HUMAN CONTROL MODEL OF THE SKATEBOARD

Human Control of the Skateboard

In order to design a human control for the skateboard, researches were carried out on the Biomechanics topic of human postural control, i.e. the ability of maintaining the balance. The latter is based on the pieces of information coming from three systems: visual, vestibular and somatosensory (see [13]). The visual system provides information from the eyes in the absolute frame of reference. The vestibular system provides information about head position and acceleration in the absolute frame of reference through the inner ear vestibulum. The somatosensory system provides information about the position of the center of pressure under the feet.
In [12] David Peterka studied the postural control on subjects standing on an oscillating platform. He experimentally demonstrated that the postural control can be modeled through a sensory reweighting system. This means that the relevance of every sensory system changes with the external perturbation, accounting in this way for the nonlinearity of the human control. For low disturbance amplitudes the balance task relies more on the somatosensory system, while for higher disturbances the relevance of the vestibular system becomes greater. The control of the human balance consists of a torque exerted at the ankles level, which is made of two contributions: an **Active Torque**, based on the neuromuscular control, and a **Passive Torque**, result of the leg muscles intrinsic features.
The control model designed for the skateboard is shown in Fig.5. The core of the model is the skateboard-rider mechanical system, which contains the equations of motion (25) and takes as input the ankles torque T_B and gives as output the angle ϕ and γ. The outputs are elaborated by the sensory systems: the visual and vestibular systems act on the same angle ϕ, which is the skater COM angle in the absolute frame of reference, while

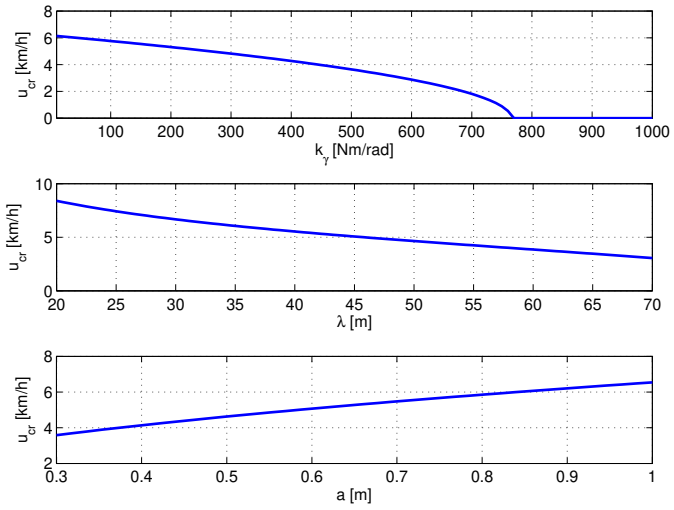

FIGURE 6: STIFFNESS k_γ, PIVOT ANGLE λ AND WHEELBASE a INFLUENCE ON CRITICAL SPEED

the somatosensory system acts on the skater angle relative to the board $\phi - \gamma$. The red boxes contains the weighting factor W_v and W_s, representing the sensory reweighting system, such that $W_v + W_s = 1$. The error from the equilibrium position elaborated by the sensory reweighting system enters then in a PD controller, with K_p as the proportional term and K_d as the derivative term, and determines the active torque T_a. The latter is summed to the passive torque T_p, which depends on the muscular ankles stiffness K and damping C, in order to give the total ankles torque $T_B = T_a + T_p$. The total ankle torque can then be written as:

$$T_B = K_p(\phi - W_s\gamma) + K_d(\dot{\phi} - W_s\dot{\gamma}) + K(\phi - \gamma) + C(\dot{\phi} - \dot{\gamma}) \quad (26)$$

The values of the PD controller terms were taken from Peterka's paper [12] as $K_p = 1000$ Nmrad^{-1} and $K_d = 100$ Nmsrad^{-1}. Concerning the passive torque, the value of the ankle passive stiffness was determined by Peterka to be $K = 94$ Nmrad^{-1}. Peterka also determined the value of C. However, its entity suggested him that the passive damping C may contribute more to overall damping when the surface is fixed than when it is moving. Therefore, considering the mobility of the skateboard, we will use the value found by Maura Casadio in her study [14] on the ankles impedance. The value is then assumed to be $c = 5.8$ Nmsrad^{-1}.

STABILITY ANALYSIS

A parametric stability analysis with the poles location method was carried out to investigate the influence of different skateboard setups. The Laplace transformation is applied to the linearized equations (23) and (25) to obtain the system characteristic polynomial, whose solutions determine its poles, thus its stability.

All the figures show the poles going from a blue color to a red color as the chosen parameter value increases.

The data of the chosen skateboard - rider configuration are shown in Table 1 and they represent an average skateboard set-up and an average human body in a standing position and were taken from previous studies and anthropometry sources (see [3, 10, 11]).

Model 1 - Results

The stability of the skateboard-rider model is studied by varying different parameters, while maintaining fixed all the others.

The first considered parameter is the longitudinal speed u.

Figure 7 shows the eigenvalues position for a symmetric skateboard-rider configuration ($\lambda_f = \lambda_r$, $\mu = 1$, $p = 0$ m): at low speeds the system has a couple of real symmetric eigenvalues, thus it's unstable. With higher speeds the system has a couple of purely imaginary eigenvalues and shows a marginally stable oscillatory behavior, with increasing frequency. The latter aspect is due to the fact that the centripetal restoring torque, represented by the γ-term of equation (23), increases with the square of the speed, increasing the overall stiffness of the system.Thus the speed has a stabilizing effect,as it happens in bikes and motorbikes (see [8]). The characteristic equation of the model is of the form $A_0 s^2 + B_0 s + C_0 = 0$ and the critical speed, above which the motion becomes stable, corresponds to the value of u for which its discriminant $\Delta = B_0^2 - 4A_0C_0 = 0$

In Fig.6 are shown the changes in critical speed due to the spring torsional stiffness k_γ, the wheelbase a and the pivot angles λ. The critical speed u_{cr} becomes lower as k_γ become higher, until $u_{cr} = 0$. This happens when, $C_0 = 0$ for $u = 0$, thus when $k_{\gamma_{cr}} = g(m_R L + m_B h)$. Over this value, the skateboard is

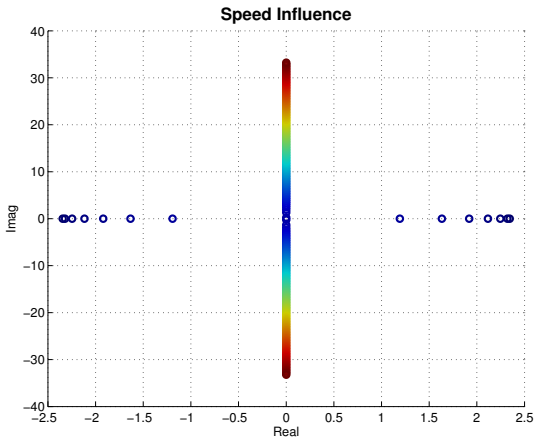

FIGURE 7: POLES LOCATION FOR SPEED $0 < u < 72km/h$

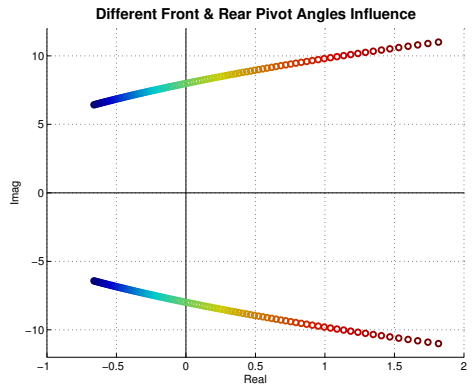

FIGURE 8: PIVOT ANGLES DIFFERENCE INFLUENCE ON STABILITY
$\lambda_f = 45°$, $25° < \lambda_r < 75°$, $u = 18\,\text{km/h}$

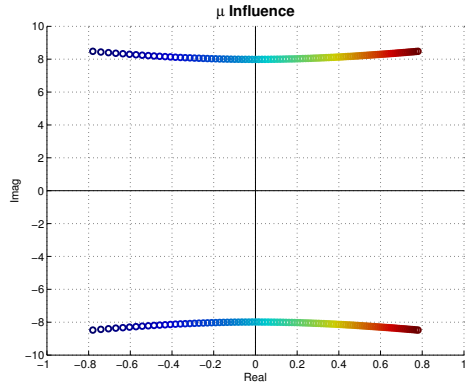

FIGURE 9: TRUCKS TIGHTENING INFLUENCE ON STABILITY
$0.5 < \mu < 2$, $u = 18\,\text{km/h}$

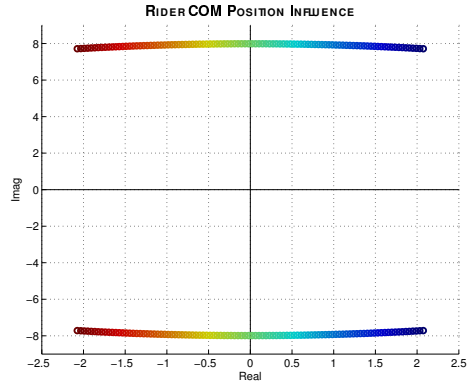

FIGURE 10: RIDER INFLUENCE ON STABILITY
$-0.1\,m < p < 0.1\,m$, $u = 18\,\text{km/h}$

marginally stable at every speed.
If now we consider an asymmetric skateboard-rider configuration, i.e. $\lambda_f \neq \lambda_r$ or $\mu \neq 1$ or $p \neq 0$, we can study the influence of these parameters. Concerning the trucks pivot angles, usually they are the same for the front and rear truck.
If we consider that the front and rear trucks are different we can fix the value of one of the two and let the other vary. This situation is represented in Fig.8: it shows that if $\lambda_f > \lambda_r$ the system is stable while if $\lambda_f < \lambda_r$ the system becomes unstable. However, using different pivot angles is not very widespread among skaters.
A simpler way of acting on the trucks is to adjust the kingpin bolt tightening level. The latter aspect was modeled through the coefficient $\mu = k_{\gamma_f}/k_{\gamma_r}$. Fig.9 shows how the stability is affected by this parameter: the skateboard-rider system is stable for $\mu < 1$, while it becomes unstable for $\mu > 1$.
As far as the position of the rider on the board p is concerned, the latter is shown to be a key parameter for the skateboard stability. Figure 10 shows that, if the rider shifts his weight in the front of the vehicle, the system is stable, otherwise the system becomes unstable.
Except for these three parameters which can lead to an asymmetric configuration, the other skateboard and rider parameters, such as the wheelbase a, the trucks overall stiffness k_γ and the COM height on the board l have no effects on the system stability. In fact their effect is only to increase or decrease the oscillation frequency, as it happens for the speed in Fig.7. Further investigation of these parameters will be offered in the human controlled skateboard of Model 2.
The results obtained from the stability study of the linearized system were then verified by solving the nonlinear full system (9) by imposing a small initial board tilt angle perturbation γ_0 and a an initial longitudinal speed u_0. The results are shown in Fig.11: Fig.11a shows the system time response of a marginally stable skateboard-rider configuration, while Fig.11b shows the system response for an unstable skateboard-rider configuration at the same speed $u_0 = 18\,\text{km/h}$.

Model 2 - Results

To analyze the system of equations (25), the ankles torque shown in Eq.(26) was replaced in the system and the Laplace transform was applied, obtaining:

$$\begin{bmatrix} A_1 s^2 + B_1 s + C_1 & A_2 s^2 + B_2 s + C_2 \\ A_2 s^2 + B_3 s + C_3 & A_3 s^2 + B_4 s + C_4 \end{bmatrix} \mathscr{L} \begin{bmatrix} \gamma \\ \phi \end{bmatrix} = \begin{bmatrix} 0 \\ 0 \end{bmatrix} \qquad (27)$$

The characteristic equation is then a quartic equation. The main task is to analyze the stability of the human control and in particular of the sensory reweighting system. In [12], David Peterka demonstrated that that, for low perturbations of his motion board (0.5°), the sensory weight distribution is the following: 50% somatosensory and 50% visual+vestibular. Instead, for larger amplitude perturbations (8°), the sensory weight distribution is

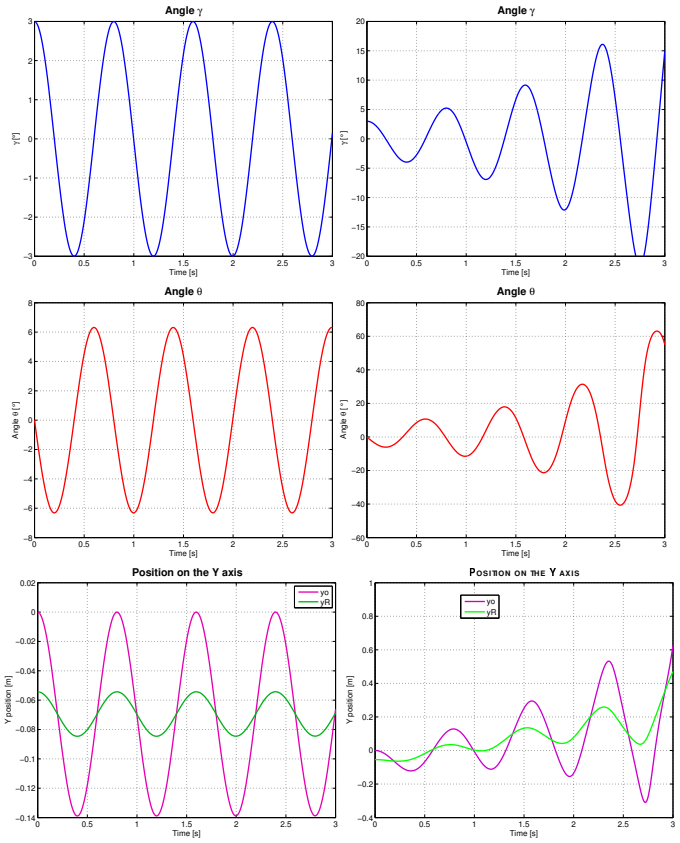

(a) Marginally Stable (b) Unstable

FIGURE 11: NONLINEAR SYSTEM RESPONSE
($\gamma_0 = \pi/70$,$u_0 = 18$Km/h)

15% somatosensory and 85% visual+vestibular. Thus, considering this aspect, we analyzed several weighting factors situations. Figure 12 shows two different situations of weighting factors distribution. Figure 12a shows that, for a somatosensory weighting factor $W_s = 0.5$, the human control is stable at every speed. Instead, Fig.12b shows that, for $W_s = 0.15$, at a certain point, the real part of a couple of eigenvalue becomes positive and the system become unstable. The value of the speed for which the latter happens is called critical wobble speed u_{cr_W}. Figure 13 shows the dependency between the somatosensory weighting factor W_s and the critical wobble speed. It can be seen that, under a certain value of W_s, the speed wobble becomes possible and the speed at which it happens decreases with W_s. In particular it can be said that, if the weight of the somatosensory system is larger than 30%, the speed wobble instability can't take place.

At this point, assuming a symmetric skateboard-rider configuration, the parameters whose influence on the system stability of Model 1 was uncertain will be analyzed in this context. Figure 14 shows the influence of several parameters on the critical wobble speed. It can be said that the critical wobble speed u_{cr_W} increases if the overall truck stiffness k_γ or the wheelbase a increases. On the other side, the critical wobble speed decreases

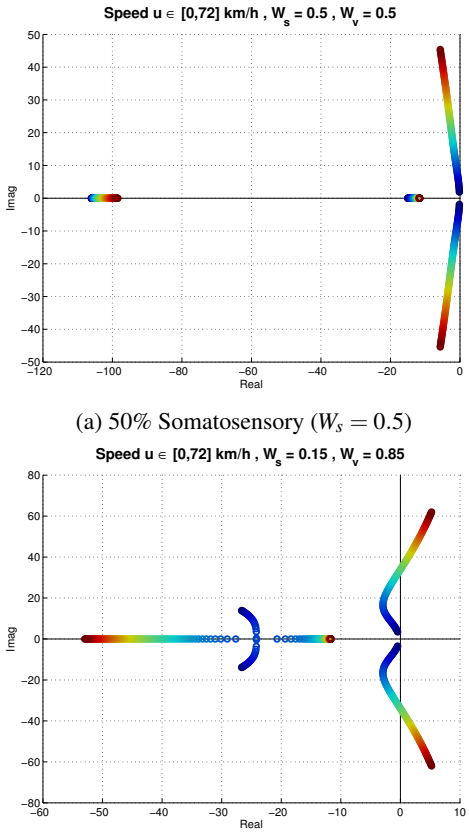

(a) 50% Somatosensory ($W_s = 0.5$)

(b) 15% Somatosensory ($W_s = 0.15$)

FIGURE 12: HUMAN CONTROL STABILITY FOR DIFFERENT SENSORY WEIGHTING FACTORS
$0 < u < 72km/h$

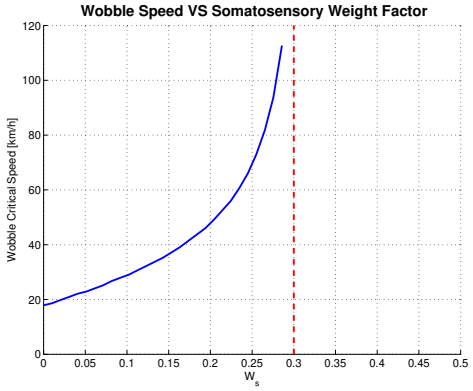

FIGURE 13: WOBBLE CRITICAL SPEED DEPENDENCY ON SOMATOSENSORY WEIGHTING FACTOR

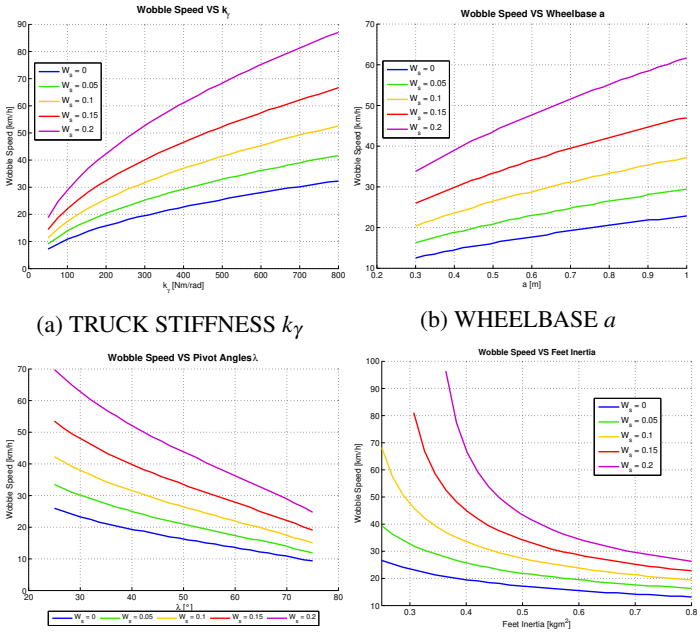

(a) TRUCK STIFFNESS k_γ

(b) WHEELBASE a

(c) PIVOT ANGLES λ

(d) FEET INERTIA I_{fx}

FIGURE 14: SKATEBOARD-RIDER PARAMETERS INFLUENCE ON WOBBLE CRITICAL SPEED FOR DIFFERENT VALUES OF W_s

when the pivot angle $\lambda_f = \lambda_r$ or the feet inertia I_{fx} increases. The latter parameter has been considered because the position of the feet on the board can be changed: in fact, if we consider a professional skater position on the board at high speed, the feet are positioned longitudinally on the board center line. In this way the feet inertia around the x-axis I_{fx} is reduced.

The effect of the different parameters on the critical wobble speed are important because they show that, the same parameters whose influence on Model 1 was not clear, are instead important from a human postural control point of view.

The results obtained from the stability analysis of the human control of the skateboard were then verified on the nonlinear full system by imposing an initial perturbation of the board tilt angle γ_0 and an initial speed u_0. Figure 15 shows the time response for two different configurations with different wobble critical speed. It can be seen that, higher the critical wobble speed, higher the oscillation frequency of the wobble instability. The frequency range of the instability is between 4 and 9 Hz.

DISCUSSION

The stability analysis on the two skateboard-rider models show different results. Model 1 showed that the there is a critical speed above which the motion is marginally stable if the skateboard-rider configuration is symmetric, i.e. when $\lambda_f = \lambda_r$, $\mu = 1$, $p = 0$. If the configuration is not symmetric, the system can become stable or unstable. By varying one parameter at a time has been discovered that the skateboard is stable over the critical speed when $\lambda_f > \lambda_r$, i.e. the front truck pivot angle is greater than the rear one; when $\mu < 1$, i.e. the rear truck is more tighten then the front one; and when $p > 0$, i.e. the rider COM is shifted more in the front of the vehicle. In the opposite cases, instead,the skateboard becomes unstable. Concerning the wobble, we were expecting an instability arising with speed increase, but in the obtained results there is no trace of such behavior. Furthermore, considering that the skateboard parameters k_γ, λ and μ can't be changed during the motion, the skateboard will always be either in a stable or unstable configuration.The only aspects that can be changed during the motion are the position p and the height l of the rider COM. The most important parameter between the two is the position p. Looking at professional long-boarders, they try to shift their weight in the front as much as possible and their COM as low as possible. In fact, as demonstrated by a few wobble videos, if the weight is shifted in the back even for a short moment, the wobble occurs and in most cases the

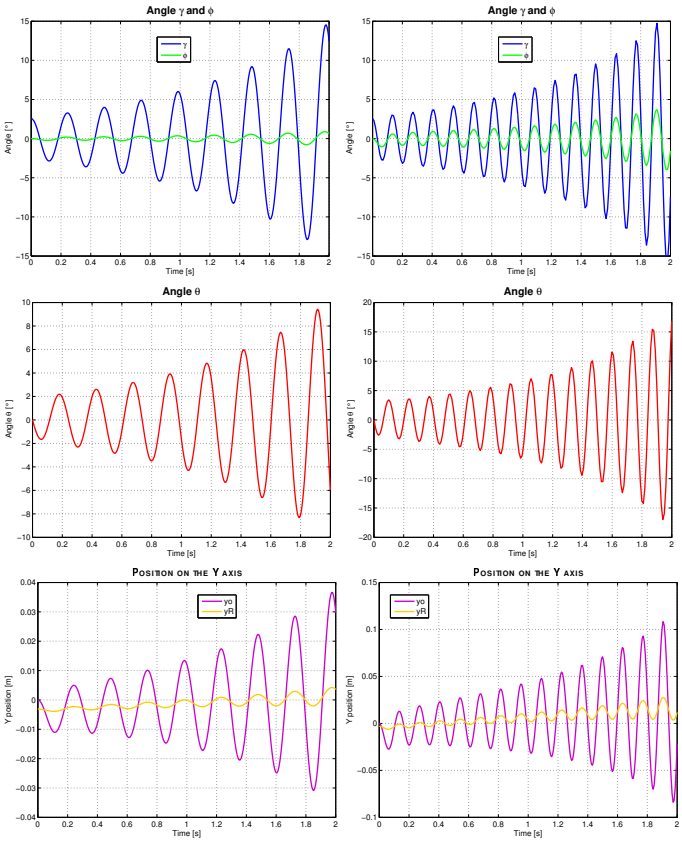

(a) $W_s = 0$, $u_0 = 20$ km/h

(b) $W_s = 0.2$, $u_0 = 55$ km/h

FIGURE 15: NONLINEAR SYSTEM RESPONSE MODEL 2 $\gamma_0 = \pi/70$

rider loses the control of the vehicle. However, if the skateboard-rider is in an unstable configurations, this doesn't mean that the rider can't control the vehicle, it will only be more difficult as the speed increases. For these reasons a human control was applied on the skateboard in Model 2. The results demonstrate that the speed wobble is due to the sensory reweighting system of the human postural control, and in particular to the loss of relevance of the somatosensory system. In fact, under a certain value of the somatosensory weigthing factor, it's possible to have a critical wobble speed, above which the human control becomes unstable. However, the evolution of the weighting factors can be very different from person to person and even within the same person, and it depends on many aspects, such as experience, training, concentration, intrinsic abilities to maintain the balance and so on. For example, a professional skater will be able to maintain the somatosensory weighting factor higher than a beginner skater for the same external perturbations. Therefore, the speed wobble effect is due in part to the skateboard setup, but in a major part to the rider skills in maintaining its balance.

Furthermore, the results of the parametric stability analysis have pointed out that the human postural control is influenced by several skateboard parameters such as the overall torsional truck stiffness k_γ, the wheelbase a and the trucks pivot angle λ. In order to increase the wobble critical speed, the skater should use longer wheelbase skateboards, tighten more the trucks and use trucks with low pivot angles. Moreover, also the feet inertia has been evaluated as a very influential parameter, and the rider should put them in a longitudinal position instead of perpendicularly. However, by doing this, the ability to turn is lowered and the available base area in which the COM projection has to fall in order to maintain the equilibrium is lower. Therefore the rider should also lower its COM on the board.

CONCLUSION

The equations of motion of two models of skateboard were obtained through Lagrange energy method and numerically solved in MATLAB®. A human postural control was implemented on the second model and the stability of the two systems evaluated through a parametric analysis in order to investigate the so called *speed wobble* instability. Model 1 showed that there are stable and unstable skateboard-rider configurations, but they don't show a clear dependency on the speed.

Model 2 demonstrates that the speed wobble instability depends on the sensory reweighting system of the human postural control and that the value of the critical wobble speed varies according to skateboard and rider parameters. The results seem to confirm skaters beliefs and opinions about the speed wobble. Therefore, even if it was demonstrated that the speed wobble depends on the rider skills, the factors that influence the instability were discovered and theoretically demonstrated.

In order to validate the theoretical results obtained in this paper, a series of experiments will be needed.

REFERENCES

[1] M. Hubbard, *Lateral Dynamics and Stability of the Skateboard.* Journal of Applied Mechanics. 1979.Vol.46

[2] M. Hubbard.*Human Control of the Skateboard.* Journal of Biomechanics. 1980.Vol.13.

[3] A. V.Kremnev,A. S.Kuleshov, *Nonlinear Dynamics and Stability of a Simplified Skateboard Model.* 2007.

[4] Y. G. Ispolov, B. A. Smolnikov, *Skateboard Dynamics* Computer Methods in Applied Mechanics and Engineering.1996.Vol.131

[5] A. E. Osterling, *On the Skateboard, Kinematics and Dynamics*.School of Mathematical Sciences, University of Exeter, UK. 2004.

[6] R. N. Jazar, *Vehicle Dynamics. Theory and Application*.2nd Edition, Springer. Chapter 7, Pages 418-434. 2014.

[7] K. Janschek, *Mechatronics Systems Design. Methods, Models, Concepts*, 1st Edition, Springer. 2011.

[8] J. V.Ringwood, R. Feng, *Bicycle Wheel Wobble* International Conference on Informatics in Control, Automation and Robotics. 2007.

[9] R.S. Sharp, D. J. N. Limebeer, *On Steering Wobble Oscillations of motorcycles*Journal opf Mechanical Engineering Sciences. 2004.

[10] D. A. Winter, *Biomechanics and Motor Control of Human Movement*. Fourth Edition. Wiley.

[11] I. P. Herman, *Physics of the Human Body*. First Edition. Springer. 2008.

[12] R. J. Peterka, *Sensorimotor Integration in Human postural Control*. Journal of Neurophysiology, Vol. 88, 2002.

[13] T. Mergner, F. Hlavacka, *Multisensory Control of Posture*. Springer, 1995. pp 281-288.

[14] M. Casadio, P. G. Morasso, V. Sanguineti, *Direct measurement of ankle stiffness during quiet standing: implications for control modelling and clinical application* Gait and Posture.Vol 21, 2005.

[15] A. Ishida, T. Masuda, H. Inaoka, Y. Fukuoka *Stability of the human upright stance depending on the frequency of external disturbances* Medical and Biological Engineering and Computing. 2007.

[16] J. R. Chagdes, S. Riedtdyk, J. M. Haddad, *Dynamic stability of a human standing on a balance board*, Journal of Biomechanics, Vol. 46, 2013.